



# Influences of Blanching and Freezing Pretreatments on Moisture Diffusivity and Quality Attributes of Pumpkin Slices During Convective Air-Drying

Yasumasa Ando<sup>1</sup> · Tomoya Okunishi<sup>2</sup> · Hiroshi Okadome<sup>2</sup>

Received: 11 April 2019 / Accepted: 23 August 2019 / Published online: 2 September 2019  
© Springer Science+Business Media, LLC, part of Springer Nature 2019

## Abstract

In this study, the relationship between moisture diffusivity in convective air-drying and cellular structure through blanching and freezing pretreatment and quality attributes of dried pumpkin slices were evaluated to obtain necessary information for designing appropriate drying and pretreatment conditions. The results suggest that the loosely bound structure of cell walls due to blanching and pores in the tissue formed by ice crystals during freezing increased moisture diffusivity. In addition, the functional and structural damage of cell membranes by the pretreatments, shown by the electrical impedance analysis, is likely involved in moisture diffusivity during drying. In particular, the sample pretreated by both blanching and freezing showed significantly higher values of moisture diffusivity compared to other samples. With regards to quality attributes, a decrease in color lightness due to starch gelatinization during blanching dramatically affected the color characteristics of the dried product. Starch gelatinization due to blanching and the formation of pores during freezing significantly influenced the structure of the samples after drying, which affected the rehydration rates and mechanical properties.

**Keywords** Convective air-drying · Pumpkin · Blanching · Freezing · Moisture diffusivity · Cellular structure

## Introduction

Pumpkin is one of the most important crops cultivated and consumed throughout the world, it is recognized as a highly nutritious foodstuff due to its high content of nutrimental and bioactive components including polysaccharides, carotenoids, vitamins, dietary fiber, minerals, vitamins, and other substances beneficial to human health (Yang et al. 2007; de Escalada Pla et al. 2007; Jacobo-Valenzuela et al. 2011; Caili et al. 2006). Pumpkins are often distributed as both raw vegetables and processed products such as frozen, pureed, precooked, or dried ma-

terials to increase their storage stability and usability (Gonçalves et al. 2011; Gliemmo et al. 2009; Provesi et al. 2011; Sojak and Głowacki 2010; Nawirska et al. 2009). Among these forms of processing, drying is the most classical method of food preservation for extending shelf-life, creating a lighter weight for transportation, and taking up less space during storage (Dandamrongrak et al. 2002). Despite the development of newer drying techniques, most vegetables are still air-dried because this method of dehydration remains the simplest and most economical (Mazza 1983). However, air-drying has the disadvantages of a longer drying time during the falling rate period, low energy efficiency (Orikasa et al. 2018), and subsequent quality deteriorations such as color fading, browning, and loss of nutrients (Krokida et al. 1998; Liu et al. 2014; Guiné and Barroca 2012; Horuz et al. 2017). Therefore, a large amount of data have been previously reported which estimate moisture diffusivity and the modeling of moisture content changes during the convective drying process of fruits and vegetables such as

✉ Yasumasa Ando  
yaando@affrc.go.jp

<sup>1</sup> Institute of Vegetable and Floriculture Science, NARO, 360 Kusawa, Anou, Tsu, Mie 514-2392, Japan

<sup>2</sup> Food Research Institute, NARO, 2-1-12 Kannondai, Tsukuba, Ibaraki 305-8642, Japan

pumpkins (Doymaz 2007; Molina Filho et al. 2016; Guiné et al. 2012), tomatoes (Hawladar et al. 1991), kiwifruit (Orikasa et al. 2008; Simal et al. 2005), and carrots (Liu et al. 2014; Doymaz 2004) to optimize drying conditions to improve efficiency.

In these ongoing studies, it has been shown that pretreatments such as blanching and freezing are effective in improving drying efficiency (Lewicki 1998; Mazza 1983; Dandamrongrak et al. 2002; Eshtiaghi et al. 1994) and suppressing the increase in sample temperature and preventing the structural deformation (Tatemoto et al. 2016; Ando et al. 2019a, b) of fruits and vegetables. Nieto et al. (1998) investigated the drying characteristics of apples after blanching and suggested that the degradation of the middle lamella and hemicellulosic polysaccharides also affects the drying rate of fruits and vegetables. The high drying rates of prefrozen samples are attributed to the high moisture transfer rates in the tissues due to the remarkable disorder of the cell wall structure caused by the formation of ice crystals during freezing (Lewicki 1998; Tatemoto et al. 2016). Furthermore, previous studies claim that destruction of the cell membrane structure and the modification of membrane permeability as a result of freezing pretreatment also increase the drying rate (Vaccarella et al. 1974; Ando et al. 2016). Therefore, the state of the cell wall and cell membrane structures should be investigated to clarify the mechanism that causes changes in drying rates due to pretreatments. It has been reported that the blanching or freezing-thawing pretreatments are effective in facilitating moisture transport within the sample tissues of pumpkins during drying (Arévalo-Pinedo and Murr 2007). However, the relationship between structural changes in cells and the moisture transport phenomenon has not been clarified.

In this study, observations of cell wall structures and electrical impedance analysis to characterize cell membrane states were applied to evaluate the changes in cellular structures by blanching and freeze-thaw pretreatments in pumpkin slices. These outcomes were then compared with estimated moisture diffusivity during convective air-drying. The dried products are sometimes used as an additive for instant soups, breads, and cakes after powdering, but are often used as a cooking ingredient after rehydration. Therefore, evaluation of rehydration characteristics and quality attributes after rehydration can be useful for the quality design of the last products. In our study, internal structures, rehydration characteristics, colors, and mechanical properties of the samples were evaluated to investigate the influence of the pretreatments on the quality attributes of the dried products. The results obtained enable a greater understanding of the drying processes which will be beneficial for designing appropriate drying and pretreatment conditions.

## Materials and Methods

### Sample Preparation

Pumpkins (*Cucurbita maxima*) of the cultivar Kofuki were obtained from a local market and used for experiments within 7 days of purchase. Kofuki is a mealy type of pumpkin with relatively high starch and sucrose contents (Cumarasamy et al. 2002). The initial moisture contents of the pumpkins were gravimetrically determined to be  $5.377 \pm 0.017$  on a dry basis (g/g) from an average of eight samples. The flesh of the pumpkin was shaped into a discoid shape with a diameter of 20.5 mm and a thickness of 3.5 mm. Four types of samples, fresh (non-treated), blanched, fresh-frozen, and blanched frozen, were used for drying. For the blanching procedure, the cylindrical sample was heated in boiling water for 40 s then immediately cooled in iced water. The sample's temperature was maintained at 25 °C in an incubator (CN-25C; Mitsubishi Electric Engineering Ltd., Tokyo, Japan) for 1 h before drying. For the freezing procedure, the sample was wrapped in plastic film and stored in a freezer (HRF-90XT; Hoshizaki Corp., Aichi, Japan) at -20 °C for more than 4 h, then thawed in the incubator at 25 °C for 3 h.

### Drying Procedure and Calculation of Effective Moisture Diffusivity

The measured room temperature and relative humidity were approximately 20 °C and 49%, respectively. During convective air-drying, samples were placed in a drying chamber (DN-42; Yamato Scientific Co., Ltd., Tokyo, Japan) at controlled temperatures of 40 °C, 60 °C, and 80 °C. The relative humidity in the chamber had been kept below 20% through the drying. The air velocity in the chamber was  $1.5 \pm 0.1$  m/s on average throughout continuous measurements over 3 min. After specified drying times, the sample was taken out of the chamber and weighed. The moisture content was calculated from both the initial moisture content and the mass.

The moisture transport phenomenon during drying is often described by using Fick's diffusion equation. An analytical solution in the case of drying a plane sheet of thin layer assuming one-dimensional moisture transport can be developed as follows (Crank 1975):

$$\frac{M-M_e}{M_0-M_e} = \frac{8}{\pi^2} \sum_{n=0}^{\infty} \frac{1}{(2n+1)^2} \exp\left\{-\frac{(2n+1)^2 D \pi^2 t}{4l^2}\right\}, \quad (1)$$

where  $M$ ,  $M_e$ , and  $M_0$  denote the moisture content, the equilibrium moisture content (equilibrium value of the moisture content determined by air temperature and relative humidity), and the initial moisture content on a dry basis, respectively.  $D$  denotes the effective diffusion coefficient ( $\text{m}^2 \text{s}^{-1}$ ),  $l$  denotes the half thickness of the sample slice (m), and  $t$  denotes the

time (s). Constants  $D$  and  $M_e$  were determined by fitting Eq. (1) to the averaged values of six samples using the least squares method using the software (MATLAB R2018a, The MathWorks, Inc., Natick, USA). Thirty terms of the series were used in the calculation which was sufficient for the convergence. The root mean squared error was calculated as an index of the goodness of fit.

### Electrical Impedance Analysis

The electrical impedance analysis, widely used to estimate the physiological status of various biological tissues (Zhang and Willison 1992; Zhang et al. 1993; Ando et al. 2014; Watanabe et al. 2018), was applied to evaluate cell membrane damage in the samples before and after each pretreatment. The impedance magnitudes  $|Z|$  ( $\Omega$ ) and phase differences  $\theta$  (rad) of the samples were measured at 81 points (logarithmic frequency intervals) over a frequency range from 50 Hz to 5 MHz using an impedance analyzer (IM3570, HIOKI E.E. Corp., Nagano, Japan). The electrodes were penetrated from a side of the sample disk with a distance of 10 mm between the electrodes. The electrodes were connected to the impedance analyzer via coaxial cables. The sample temperature was maintained in an incubator at 25 °C, and the test was carried out at a room temperature of 25 °C. The measured impedance data were analyzed using the equivalent circuit model for cellular tissues, as previously described (Ando et al. 2014, 2017). The resistance of the extracellular fluid,  $R_e$ , the resistance of the intracellular fluid,  $R_i$ , and the capacitance of the cell membrane,  $C_m$ , were all individually calculated through this model. Detailed procedures for these analyses are described in a previous study (Ando et al. 2017).

### Scanning Electron Microscopy

Fresh and pretreated samples were studied via scanning electron microscopy (SEM) to evaluate the cell wall adhesion of tissue samples. The centers of the samples were cut with a sharp knife into small blocks approximately 3.5 mm wide and 1 mm thick, before being rapidly frozen in liquid nitrogen and freeze-dried. The cross-sectional surfaces of the freeze-dried blocks were sputter-coated with gold in a sputter coater (JFC-1500; JEOL Ltd., Tokyo, Japan). These cross-sections were then observed using an SEM (JSM-5600LV; JEOL Ltd.) at an accelerating voltage of 5 kV under high vacuum conditions. The internal structures of the samples after drying were also observed. Small blocks with approximately 2 mm sides were cut with a sharp knife from the center of the dried samples. The cross-sectional surface was then observed in the same manner as previously described.

### Color Measurements

A color-difference meter (CR-300, Minolta Co., Ltd., Tokyo, Japan) was used to measure the colors of the sample surfaces during drying. After specified drying times, samples were taken out of the chamber and values of a color lightness ( $L^*$ ), redness/greenness ( $a^*$ ), and yellowness/blueness ( $b^*$ ) of both sides of the samples were measured and averaged. As indices of color characteristics, the chroma,  $C^*$ , and the hue angle,  $h$ , were calculated via the following equations, respectively:

$$C^* = \sqrt{(a^*)^2 + (b^*)^2}, \quad (2)$$

$$h = 180 \tan^{-1} \left( \frac{b^*}{a^*} \right) / \pi. \quad (3)$$

### Rehydration Characteristics

Each dried sample was immersed in 200 mL of distilled water in a beaker placed in a thermostatically controlled water bath at 30 °C. After the specified rehydration times, the samples were removed from the water and wiped with absorbent paper to remove residual water from the surface. The samples were then weighed with an electric scale. The moisture content on a dry basis (g/g) was calculated from both the initial moisture content and the mass. The exponential equation, including the single rate constant as shown below, was used to characterize the rehydration behavior of the samples (Krokida and Marinos-Kouris 2003):

$$\frac{M - M_d}{M_s - M_d} = 1 - \exp(-k_r t), \quad (4)$$

where  $M_d$  and  $M_s$  denote the moisture content of the dried sample and the saturated moisture content, respectively.  $k_r$  denotes the rehydration rate constant ( $\text{h}^{-1}$ ), and  $t$  denotes the time (h). Constants  $k_r$  and  $M_s$  were determined by fitting Eq. (4) to the averaged values of experimental data using the least squares method.

### Mechanical Properties of the Rehydrated Samples

Puncture tests of the rehydrated samples were carried out using a universal testing machine (5542; Instron, Norwood, MA, USA) equipped with a 500 N load cell. The dried samples were placed on a metal base with a 10-mm diameter hole in the center. A cylindrical plunger of 3.2 mm in diameter was then inserted at a speed of 1 mm/s into the center of the flat surface of the sample until it passed through the center of the hole and completely penetrated the sample. The trigger load was set at 0.05 N. The thickness of the samples was measured using a caliper. The value of stress was calculated by dividing

the force by the cross-sectional area of the plunger. The strain was calculated by dividing the displacement by the sample thickness. Fracture stress,  $\sigma_f$  (Pa), and initial elastic modulus,  $E$  (Pa), were calculated as indices of the mechanical properties. The value of  $E$  was defined as the slope of the first linear section of the stress-strain curve. The experiments were replicated 12–14 times for each sample. The test was carried out at a room temperature of 25 °C.

## Statistical Analysis

Statistical analyses were performed using R software version 3.5.1 (R Core Team). Differences among the means were compared using a Tukey multiple range test with the analysis of variance at a significance level of  $p < 0.05$ .

## Results and Discussion

Figure 1 shows changes in moisture content versus drying time for the fresh samples. As found in previous studies, the moisture content decreased faster at higher drying temperatures, a trend that was also observed in each pretreated sample. The solid lines in Fig. 1 represent the least squares regression analysis of the model, shown as Eq. (1), showing the good agreement with the experimental data. The effective diffusion coefficient  $D$  values determined from the analysis are shown in Table 1. For each condition, the root mean squared error between the experimental and approximate data was in the range of 0.026 to 0.051. The  $D$  value of the pretreated samples tended to increase under any temperature during drying, as compared to the fresh samples. In particular, the values of the blanched-frozen samples showed the highest  $D$  values at 1.10–1.11 times higher than those of the fresh samples. The  $D$  values of the fresh-frozen samples were slightly higher than those of blanched samples at 60 °C and 80 °C, whereas those

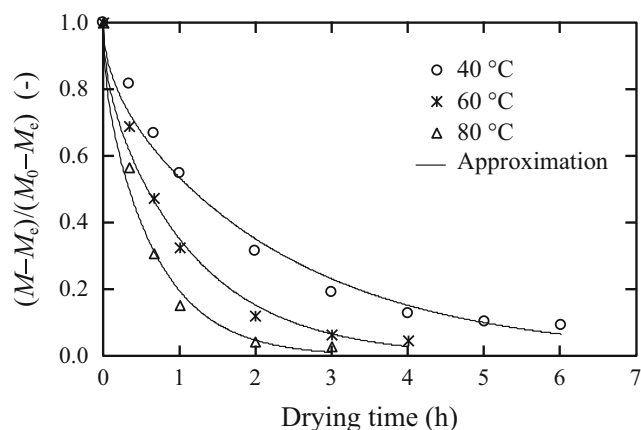


**Fig. 1** Changes in the moisture ratio during drying of the non-treated pumpkin slices. The data are mean values of 6 replicates. The solid lines represent approximations given by Eq. (1)

of the blanched and fresh-frozen samples at 40 °C showed almost the same values. These results confirm that blanching and freezing pretreatments are effective for facilitating moisture transfer in pumpkin tissues during convective air-drying, which is in line with a previous study by Arévalo-Pinedo and Murr (2007) which showed the same effect during the vacuum drying of pumpkins. In addition, the results show that the blanching-freezing pretreatments are the most effective in increasing the drying rate.

Figure 2 shows the impedance characteristics on the complex plane (Cole-Cole plot) of the fresh and pretreated samples. The impedance characteristics of the fresh sample displayed a relatively large semicircle with a diameter of 20 k $\Omega$  while those of the pretreated samples appeared markedly shrunk. It has been reported that the shrinkage of the impedance characteristics of plant tissues occurs during freezing (Wu et al. 2008; Zhang and Willison 1992) and heating (Zhang et al. 1993; Halder et al. 2011). The phenomenon is thought to be a result of structural damage to the cell membranes. Therefore, the impedance characteristic results suggest that the cell membranes in the pretreated pumpkin tissues were damaged during the blanching and freezing-thawing processes.

The measured impedance data were then analyzed with the modified Hayden model (Ando et al. 2017). The solid lines in Fig. 2 represent approximations given by the model fitted by the complex nonlinear least squares method. Note that the straight-line sections of the low-frequency areas were removed because they occurred due to the polarization phenomenon at the electrode surface (Pliquett 2010; Kalvøy et al. 2011) and are not related to the cellular structure. The measured impedance and approximate values show a good agreement for all samples, which confirms that the present model is acceptable for the application. The estimated values of the parameters in the model are shown in Table 2. The values of cell membrane capacitance,  $C_m$ , were highest in the fresh samples, while the values in other samples decreased. The high capacitance of biological tissues is thought to depend on the lipid bilayer structure of the cell membrane (Ashrafuzzaman and Tuszyński 2012). Therefore, the high  $C_m$  value of the fresh sample potentially occurred as a result of the maintenance of the membrane structures. However, the  $C_m$  values of the blanched and fresh-frozen samples decreased to 43% and 27%, respectively. A decrease in  $C_m$  has been reported in previous studies on the heating of spinach (Watanabe et al. 2017) and Japanese radish (Ando et al. 2017). This phenomenon was attributed to the thermal denaturation of phospholipids which constitute the cell membrane. It has been previously reported that  $C_m$  values decreased to 25% in apples (Ando et al. 2019b) and 53% in carrots (Ando et al. 2016) during freezing treatment at  $-20$  °C. These results are thought to stem from the formation of ice crystals during the freezing process. The lower  $C_m$  values of the fresh-frozen

**Table 1** Effective diffusion coefficient of moisture during convective air-drying of pumpkin slices estimated from Eq. (1)

| Drying temperature | Fresh                                  |          | Blanched                               |          | Fresh-frozen                           |          | Blanched-frozen                        |          |
|--------------------|--|----------|--|----------|--|----------|--|----------|
|                    | $D \times 10^{10}$ (m <sup>2</sup> /s) | RMSE (-) | $D \times 10^{10}$ (m <sup>2</sup> /s) | RMSE (-) | $D \times 10^{10}$ (m <sup>2</sup> /s) | RMSE (-) | $D \times 10^{10}$ (m <sup>2</sup> /s) | RMSE (-) |
| 40 °C              | 1.06                                   | 0.039    | 1.13                                   | 0.045    | 1.11                                   | 0.051    | 1.16                                   | 0.049    |
| 60 °C              | 2.11                                   | 0.034    | 2.20                                   | 0.034    | 2.30                                   | 0.035    | 2.32                                   | 0.032    |
| 80 °C              | 3.59                                   | 0.030    | 3.73                                   | 0.028    | 3.89                                   | 0.026    | 4.00                                   | 0.028    |

RMSE root mean squared error for the model fitting

samples suggest that freezing treatment is destructive to the cell membrane structure. The blanched-frozen samples that were stressed by both heating and freezing treatments showed the lowest  $C_m$  value (7.5% of that of the fresh sample), suggesting considerable damage to the cell membrane structure.

In healthy cells, the low electrolyte concentration of the extra-cellular fluid and high electrolyte concentration of the intracellular fluid are separated by the permselectivity of the cell membranes. Therefore, the high values of extra-cellular fluid resistance,  $R_e$ , and low values of intra-cellular resistance,  $R_i$ , of the fresh samples indicate that the cell membranes are functioning normally. In the pretreated samples, the  $R_e$  values decreased, and the  $R_i$  values increased indicating a difference in electrolyte concentration between the intra- and extra-cellular fluids. This difference occurred as a result of the cell membranes being unable to function correctly. In a study by Halder et al. (2011), the impedance of potato tissues during heating sharply declined in the temperature range of 52–60 °C. This outcome was found to be due to cell membrane

damage followed by the release of intra-cellular water into the extracellular region. Therefore, changes in the  $R_e$  and  $R_i$  values of the blanched samples observed in this study were attributed to this same phenomenon due to heating stress to the cell membranes. During the freezing process, the interior of the cells is rapidly dehydrated with ice crystal growth in the extracellular region. This stress causes the alteration of membrane transport properties (Palta 1990) resulting in fatal disruption of the cell membrane (Ando et al. 2012).

Changes in the  $R_e$  and  $R_i$  of the fresh-frozen samples can be explained by this phenomenon. The change ratio of the  $R_e$  and  $R_i$  values of blanched-frozen samples tended to increase, as with the changes in the  $C_m$  values, compared to the blanched or fresh-frozen samples. These results suggest that the cell membranes were markedly damaged in the blanched-frozen sample. Figure 3 shows the SEM images of cross-sections of the fresh and pretreated samples. Cells with an approximate 50 μm diameter in the tissues of fresh samples (Fig. 3A, a) were densely arranged. The cell walls were split, and the interiors of the cells containing starch particles of approximately 10 μm in diameter were exposed. In the fresh samples, the cell walls strongly adhered to each other, whereas the blanched samples showed a loosely bound structure of the cell walls (Fig. 3B, b), likely due to a β-elimination reaction splitting the homogalacturonan chains that primarily comprise the pectin structure (Sila et al. 2009). In the blanched sample, the cell walls were divided at the middle lamella when the tissue was cut due to this reaction. Therefore, the saclike structures of the cell walls were exposed, and the interiors of the cells were not

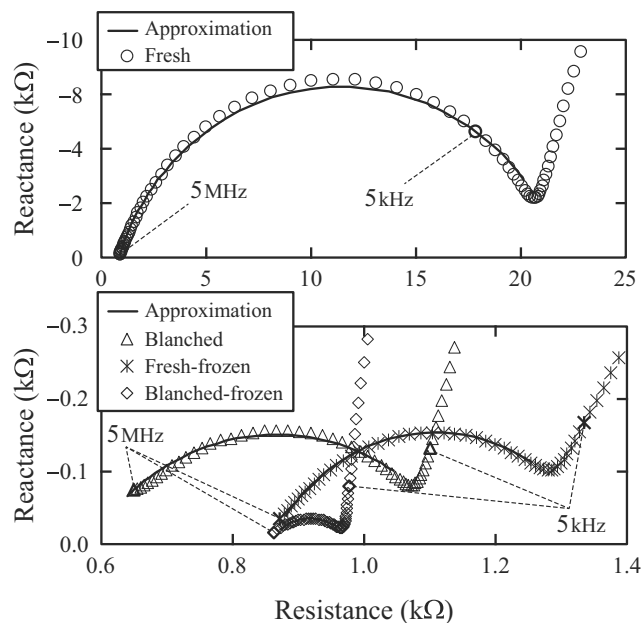


**Fig. 2** Representative Cole-Cole plots for the fresh, blanched, fresh-frozen, and blanched-frozen pumpkin slice samples. The solid lines represent approximations given by the modified Hayden model (Ando et al. 2017)

**Table 2** Equivalent circuit parameters obtained from the model fitting

|                 | $C_m$ (pF)            | $R_e$ (kΩ)                | $R_i$ (kΩ)               |
|-----------------|-----------------------|---------------------------|--------------------------|
| Fresh           | 509 <sup>a</sup> ± 8  | 22.47 <sup>a</sup> ± 0.61 | 0.80 <sup>c</sup> ± 0.03 |
| Blanched        | 219 <sup>b</sup> ± 14 | 1.39 <sup>b</sup> ± 0.03  | 2.56 <sup>b</sup> ± 0.17 |
| Fresh-frozen    | 138 <sup>c</sup> ± 17 | 1.22 <sup>b</sup> ± 0.05  | 2.03 <sup>b</sup> ± 0.14 |
| Blanched-frozen | 38 <sup>d</sup> ± 2   | 1.02 <sup>b</sup> ± 0.03  | 6.99 <sup>a</sup> ± 0.43 |

$C_m$  capacitance of cell membrane,  $R_e$  extracellular fluid resistance,  $R_i$  intracellular fluid resistance

The values of  $C_m$ ,  $R_e$ , and  $R_i$  represent the mean values of 12 replicates (± standard error). Different superscripts indicate significant differences ( $p < 0.05$ ) between the means compared by a Tukey’s multiple range test

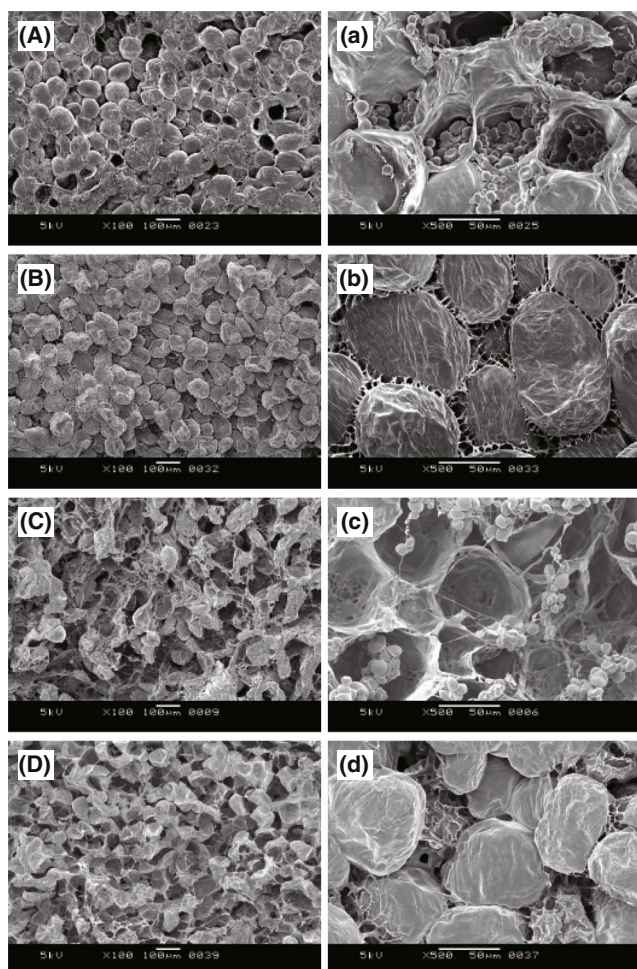


**Fig. 3** Scanning electron micrographs of cross sections of the fresh (A, a), blanched (B, b), fresh-frozen (C, c), and blanched-frozen (D, d) pumpkin slices (A, B, C, and D:  $\times 100$  images, a, b, c, and d:  $\times 500$  images)

observed. The tissues of the fresh-frozen samples showed sparse structures presumed to have occurred due to ice crystal formation during freezing (Fig. 3C, c). Although the structures are largely disrupted in the fresh-frozen samples, the separations between the cell walls as seen in the blanched samples were not observed. In the blanched-frozen samples, a sparse structure was observed as with the fresh-frozen sample, and the cell walls were largely separated compared to the blanching samples (Fig. 3D, d).

In terms of the relation of the damages to the cell membrane caused by the pretreatments and the moisture diffusivity, the samples with a higher change ratio of the parameters, i.e., with more significant damage to the cell membranes, had higher  $D$  values. This result is consistent with a previous study by Ando et al. (2012) which claims that structural and functional damage to cell membranes leads to an increase in water permeability and accelerates moisture transfer in plant tissues. In addition, it was assumed that damage to the cell walls, i.e., the separation of cell walls attributed to changes in pectin structures by heating, and physical damage due to the

growth of ice crystals during freezing also contributed to an increase in moisture diffusivity. In particular, the highest  $D$  values of the blanched-frozen samples were attributed to the marked damage to both cell membranes and cell wall structures, suggesting that blanching-freezing pretreatment is effective in increasing the drying rate and reducing the drying time required.

Figure 4 shows the changes in the color parameters, lightness  $L^*$ , chroma  $C^*$ , and Hue angle  $h$  during drying at 60 °C. The lower values of  $L^*$  and  $C^*$  of the blanched and blanched-frozen samples before drying compared to other samples are likely due to leakage of the gas spaces present in the tissue, as reported in studies on the vacuum impregnation of pears (Perez-Cabrera et al. 2011) and papayas (Yang et al. 2017). It is theorized that the internal gas expands and therefore forces its way out of the tissue during blanching. This occurrence results in the replacement of the gas phase by the liquid

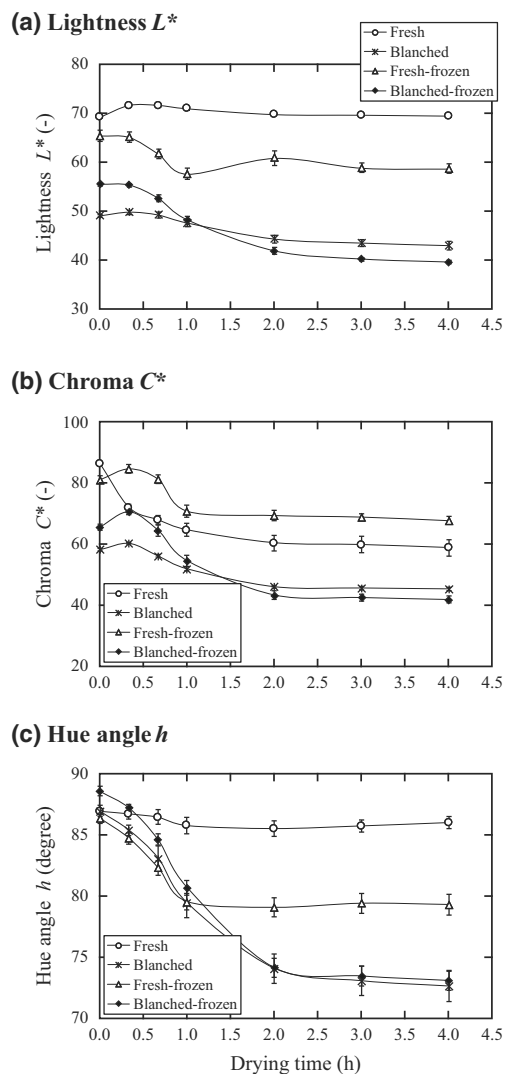


**Fig. 4** Changes in the lightness (a), chroma (b), and Hue angle (c) of pumpkin slice samples during convective air-drying at 60 °C. The data are mean values of 8 replicates. Bars denote standard error

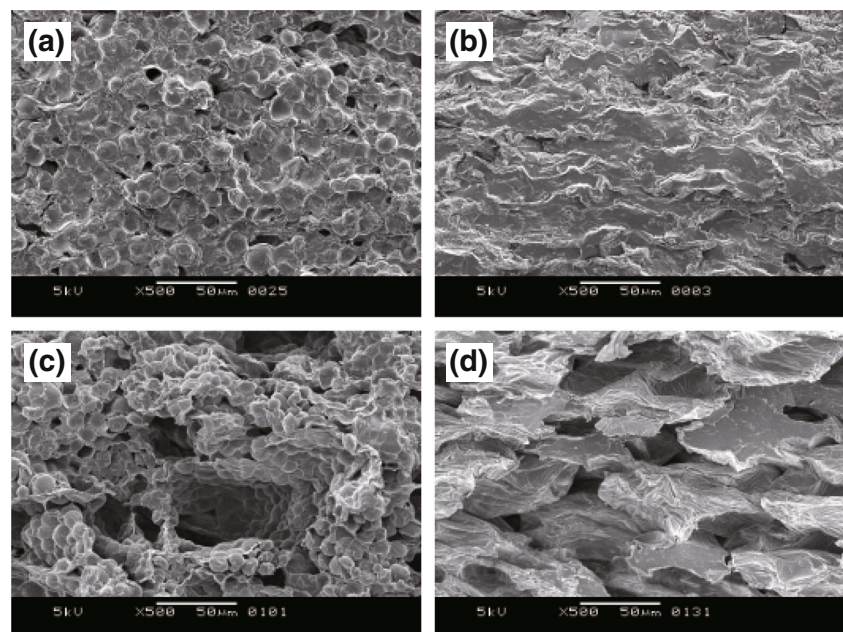
phase, inducing more homogenous refractive indices in the tissues. This event promotes light absorption against scattering resulting in the tissue samples becoming transparent with decreasing in lightness and chroma (Chiralt and Talens 2005).

Furthermore, swollen starch particles due to gelatinization during heating may have also contributed to the optical properties. The values of  $L^*$  and  $C^*$  of the fresh-frozen samples were slightly lower than those of the fresh samples due to the destruction of cellular structures and the inflow of cellular water into the intercellular spaces during freezing. The  $L^*$  values of the blanched and blanched-frozen samples tend to decrease even further from the initial low values. This result may be attributed to the high amorphous starch fractions of the gelatinized starch maintained during drying (Xiang et al. 2018) which indicates restrained light scattering and low lightness. The  $L^*$  and  $C^*$  values of the fresh-frozen and blanched-frozen samples tend to decrease more substantially than those of the fresh and blanched samples during the drying process. This result may be explained by the oxidization of carotenoids (Song et al. 2017) which is prone to occur in the frozen-thawed tissues where the cell walls and membranes are significantly destroyed (Park 1987). The fact that the decrease in the  $C^*$  value was almost depended on the decrease in the  $b^*$  value (decrease in yellowness) supports this view. The values of the hue angles  $h$  of the fresh samples were nearly constant during drying. However, the values of other samples decreased, especially for the blanched and blanched-frozen samples which showed lower values compared to the fresh-frozen samples. Decreases in hue angles during the air-drying of blanched pumpkins have been previously reported (Song et al. 2017). This phenomenon is thought to be a result of the degradation of carotenoid pigments and the formation of

brown compounds due to Maillard reactions during drying. However, in this study, subequal decreases in  $h$  values were observed even when drying at low temperatures. This result suggests that the reaction that occurs in the blanching process forms brown compounds; then, they are concentrated with drying and strongly reflected in the  $h$  values of gelatinized dried tissues with lower scattering and higher transparency. These trends of color change are similar at other drying temperatures, and they are dependent on moisture content, not drying time (data not shown).

Figure 5 shows the internal structure of the pumpkin slice samples after drying at 60 °C. In the fresh samples, structures with densely packed starch particles approximately 10  $\mu\text{m}$  in diameter are observed (Fig. 5a). Structures of the blanched samples show a smooth surface (Fig. 5b) as observed in dried starch noodles (Xiang et al. 2018). This result demonstrates the state in which gelatinized starch particles are accumulated and densely compressed by the drying shrinkage. In the fresh-frozen samples, although starch particles were observed as with the fresh samples, pores formed due to ice crystal formation during freezing were distributed throughout the inside (Fig. 5c). The blanched-frozen samples also showed a porous structure with many airspaces (Fig. 5d), though the starch particles were gelatinized entirely. Figure 6 shows changes in the moisture content during rehydration at 30 °C for each dried sample. The moisture content of the blanched-frozen samples reached its saturation at the lowest time of 1 h, while other samples required more than 3 h. The estimated values of the rehydration rate constant  $k_r$  are 0.96, 2.10, 2.25, and 7.38  $\text{h}^{-1}$  for the fresh, blanched, fresh-frozen, and blanched-frozen samples, respectively. Here, the determination coefficients for all samples are greater than 0.99, which indicates

**Fig. 5** Scanning electron micrographs of cross sections of the fresh (a), blanched (b), fresh-frozen (c), and blanched-frozen (d) pumpkin slices after convective air-drying at 60 °C



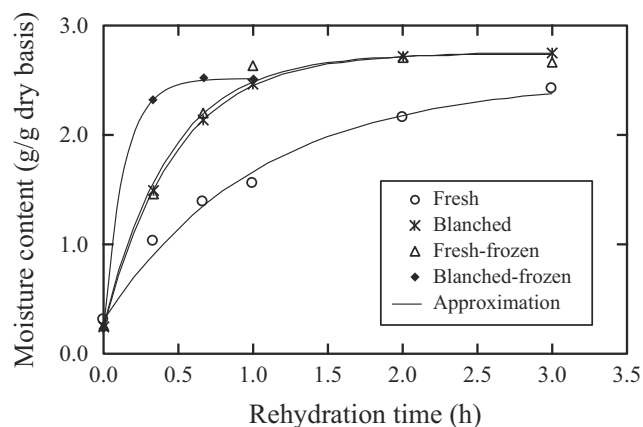


**Fig. 6** Changes in the moisture content of the pumpkin slice samples dried at 60 °C during rehydration at 30 °C. The data are mean values of 6 replicates. The solid lines represent approximations given by the exponential model shown as Eq. (4)

that the model was appropriate for explaining the rehydration phenomenon. Water can generally be absorbed more efficiently by amorphous food materials than by crystalline materials during hydration (Xiang et al. 2018). Therefore, the higher  $k_r$  values of the blanched and blanched-frozen samples could be explained by their higher amorphous starch fractions due to gelatinization during blanching. In addition, the porous internal structures of the fresh-frozen and blanched-frozen samples mean that there is a larger surface area to absorb water which may also contribute to the high values of  $k_r$ . These results show that the blanching and freezing treatments before drying are effective in increasing the rehydration rate of the dried samples.

Figure 7 shows the representative stress-strain curves by the puncture test of the fresh and pretreated pumpkin slices before drying and after drying-rehydration. Before drying, the stress of the fresh sample was significantly higher than that of pretreated samples, which is considered to be due to the integrity of the cellular structure. Although the value was decreased in the samples after drying-rehydration, the stress of the fresh sample was higher than that of other samples as before drying. Table 3 shows the fracture stress,  $\sigma_f$ , and initial modulus,  $E$ , of the samples before drying and after drying-rehydration. Before drying, the highest values of  $\sigma_f$  and  $E$  are observed in fresh samples attributable to the maintained integrity of the cell walls and cell membrane structures. However, in the blanched samples, the  $\sigma_f$  value markedly decreases (94% decrease) compared to the fresh samples, which is potentially attributable to the loosely bound structure of the cell walls, as shown in Fig. 3b, due to the degradation of pectin structures caused by heating (Sila et al. 2009). The  $\sigma_f$  value of the fresh-frozen samples also decreased purportedly due to the destruction of the cell wall structures caused by ice crystal formation during freezing and cell membrane damage demonstrated by the impedance analysis. However, the  $\sigma_f$  value of the fresh-frozen samples was slightly retained compared to the

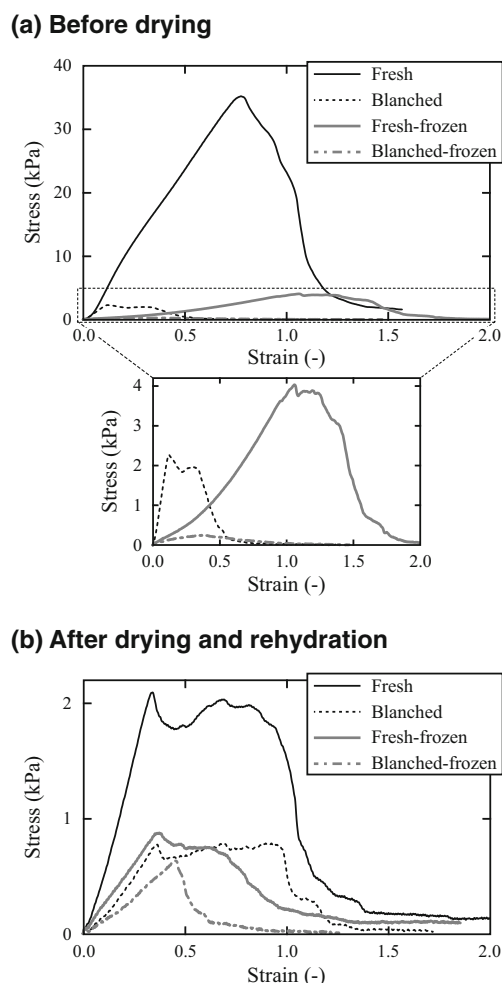


**Fig. 7** Representative stress-strain curves by the puncture test of the fresh and pretreated pumpkin slices before drying (a) and after drying at 60 °C and rehydration at 30 °C (b)

blanched samples because the dissociation of the cell walls by heating did not occur.

Conversely, the fresh-frozen sample showed a marked decrease in the  $E$  value (96% decrease). The reduction of turgor pressure due to changes in cell membrane states is a major factor for the mechanical parameters, especially the elasticity of vegetable tissues (Chassagne-Berces et al. 2009; Ando et al. 2012). Therefore, the low  $E$  value of the fresh-frozen samples can be explained through structural and functional damage to the cell membranes by freezing treatment, as suggested by the impedance analysis. The blanched-frozen samples which were subjected to heating and freezing stresses show markedly decreased values of  $\sigma_f$  and  $E$ .

As for the samples after drying-rehydration, although the fresh sample had the highest values of  $\sigma_f$  and  $E$  compared to other samples, they were significantly decreased compared to the fresh sample before drying, likely due to structural destruction during drying (Ando et al. 2014), indicating that it is difficult to restore the values by rehydration. In the blanched samples, the values of  $\sigma_f$  and  $E$  decreased to 33% and 13%,



**Table 3** Mechanical properties of the pumpkin slice samples

| Condition                                      | Fracture stress $\sigma_f$ (Pa) | Initial modulus $E$ (Pa)   |
|--|---------------------------------|----------------------------|
| Before drying                                  |                                 |                            |
| Fresh  | 36,535 <sup>a</sup> ± 1908      | 44,090 <sup>a</sup> ± 3399 |
| Blanched                                       | 2129 <sup>bc</sup> ± 114        | 16,649 <sup>b</sup> ± 1167 |
| Fresh-frozen                                   | 4607 <sup>b</sup> ± 518         | 1770 <sup>c</sup> ± 149    |
| Blanched-frozen                                | 326 <sup>c</sup> ± 18           | 1388 <sup>c</sup> ± 128    |
| After drying at 60 °C and rehydration at 30 °C |                                 |                            |
| Fresh  | 1918 <sup>a</sup> ± 143         | 7718 <sup>a</sup> ± 534    |
| Blanched                                       | 710 <sup>b</sup> ± 40           | 2174 <sup>b</sup> ± 361    |
| Fresh-frozen                                   | 722 <sup>b</sup> ± 108          | 1018 <sup>b</sup> ± 197    |
| Blanched-frozen                                | 442 <sup>b</sup> ± 39           | 1025 <sup>b</sup> ± 114    |

The values represent the mean values of 12–14 replicates ( $\pm$  standard error). Different superscripts indicate significant differences ( $p < 0.05$ ) between the means compared by a Tukey's multiple range test. The values of the samples before drying and after drying-rehydration were separately compared

respectively, through drying-rehydration treatment for the same reason. The lower value of  $E$  of the fresh-frozen sample than that of the blanched sample indicates that the formation of pores in tissues due to freezing treatment results in a further reduction in elasticity of the rehydrated sample. The values of  $\sigma_f$  and  $E$  of the blanched-frozen sample did not change before or after drying-rehydration, indicating that structural destruction occurs mostly before drying and no further mechanical change occurs during the drying-rehydration process. The results reveal that the blanching and freezing pretreatments were effective in increasing the rehydration rate of the dried materials but lead to a reduction in the parameters of mechanical properties.

## Conclusions

This study aimed to clarify the relationship between the moisture diffusivity of pumpkin slices during convective air-drying and changes in the cellular structure due to blanching and freezing pretreatments, as well as the quality attributes of the dried products. The loosely bound structure of the cell walls likely due to a  $\beta$ -elimination reaction splitting the homogalacturonan chains caused by thermal blanching was observed in blanched sample, whereas the formation of pores presumed to have occurred due to ice crystal development during freezing was observed in frozen samples, respectively. In particular, the samples treated with both blanching and freezing showed significantly destroyed structures of the cell walls. The electrical impedance analysis shows a decrease in the cell membrane capacitance and the changes in the intra- and extra-cellular fluid resistances those reflect the structural and functional damages to the membranes for the pretreated samples. This trend was remarkable in the blanched-frozen

sample, and that of blanched and fresh-frozen samples was almost the same level. The estimated value of moisture diffusivity was lowest in fresh samples at each drying temperature, potentially due to the cell wall and cell membrane structures maintaining their integrity and restraining water transfer. Among pretreated samples, the blanched-frozen samples show the highest value of moisture diffusivity at 1.10–1.11 times higher than those of the fresh samples at each drying temperature. This result suggests the structural and functional damages to the cell walls and cell membranes by the pretreatments facilitate moisture transfer increasing the drying rate.

Changes in color were found to appear predominantly in the blanched samples, and the influence of freezing was limited. This change is potentially attributed to an increase in transparency due to starch gelatinization, and the formation of brown compounds concentrated with drying. Moreover, starch gelatinization by blanching and the formation of pores during freezing greatly influenced the structures of the dried samples, resulting in increases of the rehydration rate. In particular, the rehydration rate of the blanched-frozen samples showed the highest value, 7.7 times higher compared to the fresh sample. However, significant reductions in the parameters of the mechanical properties by the pretreatments were observed in the mechanical test of the sample after drying-rehydration. These findings may be valuable in predicting drying times and quality attributes and designing appropriate drying and pretreatment conditions. The calculation of total energy spent throughout the process of pretreatment and drying and the optimization of the process conditions taking into account for the consumer acceptability of the texture and other quality attributes should be addressed in future work.

**Funding Information** This work was supported by JSPS KAKENHI Grant Number JP18K14554.

## Compliance with Ethical Standards

**Conflict of Interest** The authors declare that they have no conflict of interest.

## References

- Ando, H., Kajiwara, K., Oshita, S., & Suzuki, T. (2012). The effect of osmotic dehydrofreezing on the role of the cell membrane in carrot texture softening after freeze-thawing. *Journal of Food Engineering*, 108(3), 473–479.
- Ando, Y., Mizutani, K., & Wakatsuki, N. (2014). Electrical impedance analysis of potato tissues during drying. *Journal of Food Engineering*, 121, 24–31.
- Ando, Y., Maeda, Y., Mizutani, K., Wakatsuki, N., Hagiwara, S., & Nabetani, H. (2016). Impact of blanching and freeze-thaw pretreatment on drying rate of carrot roots in relation to changes in cell membrane function and cell wall structure. *LWT-Food Science and Technology*, 71, 40–46.

- Ando, Y., Hagiwara, S., & Nabetani, H. (2017). Thermal inactivation kinetics of pectin methyltransferase and the impact of thermal treatment on the texture, electrical impedance characteristics and cell wall structure of Japanese radish (*Raphanus sativus* L.). *Journal of Food Engineering*, 199, 9–18.
- Ando, Y., Hagiwara, S., Nabetani, H., Sotome, I., Okunishi, T., Okadome, H., Orikasa, T., & Tagawa, A. (2019a). Improvements of drying rate and structural quality of microwave-vacuum dried carrot by freeze-thaw pretreatment. *LWT-Food Science and Technology*, 100, 294–299.
- Ando, Y., Hagiwara, S., Nabetani, H., Sotome, I., Okunishi, T., Okadome, H., Orikasa, T., & Tagawa, A. (2019b). Effects of prefreezing on the drying characteristics, structural formation and mechanical properties of microwave-vacuum dried apple. *Journal of Food Engineering*, 244, 170–177.
- Arévalo-Pinedo, A., & Murr, F. E. X. (2007). Influence of pre-treatments on the drying kinetics during vacuum drying of carrot and pumpkin. *Journal of Food Engineering*, 80(1), 152–156.
- Ashrafuzzaman, M., & Tuszynski, J. (2012). Structure of membranes. In *Membrane biophysics* (pp. 9–30). Berlin: Springer.
- Caili, F. U., Huan, S., & Quanhong, L. I. (2006). A review on pharmacological activities and utilization technologies of pumpkin. *Plant Foods for Human Nutrition*, 61(2), 70–77.
- Chassagne-Berces, S., Poirier, C., Devaux, M. F., Fonseca, F., Lahaye, M., Pigorini, G., Girault, C., Marin, M., & Guillon, F. (2009). Changes in texture, cellular structure and cell wall composition in apple tissue as a result of freezing. *Food Research International*, 42(7), 788–797.
- Chiralt, A., & Talens, P. (2005). Physical and chemical changes induced by osmotic dehydration in plant tissues. *Journal of Food Engineering*, 67(1–2), 167–177.
- Crank, J. (1975). *The mathematics of diffusion* (second ed.). Oxford: Clarendon Press.
- Cumarasamy, R., Corrigan, V., Hurst, P., & Bendall, M. (2002). Cultivar differences in New Zealand “Kabocha” (buttercup squash, *Cucurbita maxima*). *New Zealand Journal of Crop and Horticultural Science*, 30(3), 197–208.
- Dandamrongrak, R., Young, G., & Mason, R. (2002). Evaluation of various pre-treatments for the dehydration of banana and selection of suitable drying models. *Journal of Food Engineering*, 55(2), 139–146.
- de Escalada Pla, M. F., Ponce, N. M., Stortz, C. A., Gerschenson, L. N., & Rojas, A. M. (2007). Composition and functional properties of enriched fiber products obtained from pumpkin (*Cucurbita moschata* Duchesne ex Poiret). *LWT-Food Science and Technology*, 40(7), 1176–1185.
- Doymaz, I. (2004). Convective air drying characteristics of thin layer carrots. *Journal of Food Engineering*, 61(3), 359–364.
- Doymaz, I. (2007). The kinetics of forced convective air-drying of pumpkin slices. *Journal of Food Engineering*, 79(1), 243–248.
- Eshtiaghi, M. N., Stute, R., & Knorr, D. (1994). High-pressure and freezing pretreatment effects on drying, rehydration, texture and color of green beans, carrots and potatoes. *Journal of Food Science*, 59(6), 1168–1170.
- Gliemmo, M. F., Latorre, M. E., Gerschenson, L. N., & Campos, C. A. (2009). Color stability of pumpkin (*Cucurbita moschata*, Duchesne ex Poiret) puree during storage at room temperature: Effect of pH, potassium sorbate, ascorbic acid and packaging material. *LWT-Food Science and Technology*, 42(1), 196–201.
- Gonçalves, E. M., Pinheiro, J., Abreu, M., Brandão, T. R. S., & Silva, C. L. M. (2011). Kinetics of quality changes of pumpkin (*Curcurbita maxima* L.) stored under isothermal and non-isothermal frozen conditions. *Journal of Food Engineering*, 106(1), 40–47.
- Guiné, R. P., & Barroca, M. J. (2012). Effect of drying treatments on texture and color of vegetables (pumpkin and green pepper). *Food and Bioprocess Processing*, 90(1), 58–63.
- Guiné, R. P. F., Henriques, F., & Barroca, M. J. (2012). Mass transfer coefficients for the drying of pumpkin (*Cucurbita moschata*) and dried product quality. *Food and Bioprocess Technology*, 5(1), 176–183.
- Halder, A., Datta, A. K., & Spanswick, R. M. (2011). Water transport in cellular tissues during thermal processing. *AIChE Journal*, 57(9), 2574–2588.
- Hawladar, M. N. A., Uddin, M. S., Ho, J. C., & Teng, A. B. W. (1991). Drying characteristics of tomatoes. *Journal of Food Engineering*, 14(4), 259–268.
- Horuz, E., Bozkurt, H., Karataş, H., & Maskan, M. (2017). Effects of hybrid (microwave-convective) and convective drying on drying kinetics, total phenolics, antioxidant capacity, vitamin C, color and rehydration capacity of sour cherries. *Food Chemistry*, 230, 295–305.
- Jacobo-Valenzuela, N., Maróstica-Junior, M. R., de Jesús Zazueta-Morales, J., & Gallegos-Infante, J. A. (2011). Physicochemical, technological properties, and health-benefits of *Cucurbita moschata* Duchesne vs. Cehualca: A review. *Food Research International*, 44(9), 2587–2593.
- Kalvøy, H., Johnsen, G. K., Martinsen, Ø. G., & Grimnes, S. (2011). New method for separation of electrode polarization impedance from measured tissue impedance. *The Open Biomedical Engineering Journal*, 5(1), 8–13.
- Krokida, M. K., & Marinos-Kouris, D. (2003). Rehydration kinetics of dehydrated products. *Journal of Food Engineering*, 57(1), 1–7.
- Krokida, M. K., Tsami, E., & Maroulis, Z. B. (1998). Kinetics on color changes during drying of some fruits and vegetables. *Drying Technology*, 16(3–5), 667–685.
- Lewicki, P. P. (1998). Effect of pre-drying treatment, drying and rehydration on plant tissue properties: A review. *International Journal of Food Properties*, 1(1), 1–22.
- Liu, Y., Wu, J., Miao, S., Chong, C., & Sun, Y. (2014). Effect of a modified atmosphere on drying and quality characteristics of carrots. *Food and Bioprocess Technology*, 7(9), 2549–2559.
- Mazza, G. (1983). Dehydration of carrots - effects of pre-drying treatments on moisture transport and product quality. *Journal of Food Technology*, 18(1), 113–123.
- Molina Filho, L., Frascareli, E. C., & Mauro, M. A. (2016). Effect of an edible pectin coating and blanching pretreatments on the air-drying kinetics of pumpkin (*Cucurbita moschata*). *Food and Bioprocess Technology*, 9(5), 859–871.
- Nawirska, A., Figiel, A., Kucharska, A. Z., Sokół-Lętowska, A., & Biesiada, A. (2009). Drying kinetics and quality parameters of pumpkin slices dehydrated using different methods. *Journal of Food Engineering*, 94(1), 14–20.
- Nieto, A., Salvatori, D., Castro, M. A., & Alzamora, S. M. (1998). Air drying behaviour of apples as affected by blanching and glucose impregnation. *Journal of Food Engineering*, 36(1), 63–79.
- Orikasa, T., Wu, L., Shiina, T., & Tagawa, A. (2008). Drying characteristics of kiwifruit during hot air drying. *Journal of Food Engineering*, 85(2), 303–308.
- Orikasa, T., Koide, S., Sugawara, H., Yoshida, M., Kato, K., Matsushima, U., Okada, M., Watanabe, T., Ando, Y., Shiina, T., & Tagawa, A. (2018). Applicability of vacuum-microwave drying for tomato fruit based on evaluations of energy cost, color, functional components and sensory qualities. *Journal of Food Processing and Preservation*, 42(6), e13625. <https://doi.org/10.1111/jfpp.13625>.
- Palta, J. P. (1990). Stress interactions at the cellular and membrane levels. *Hortscience*, 25, 1377–1381.
- Park, Y. W. (1987). Effect of freezing, thawing, drying, and cooking on carotene retention in carrots, broccoli and spinach. *Journal of Food Science*, 52(4), 1022–1025.
- Perez-Cabrera, L., Chafer, M., Chiralt, A., & Gonzalez-Martinez, C. (2011). Effectiveness of antibrowning agents applied by vacuum

- impregnation on minimally processed pear. *LWT-Food Science and Technology*, 44(10), 2273–2280.
- Pliquett, U. (2010). Bioimpedance: A review for food processing. *Food Engineering Reviews*, 2(2), 74–94.
- Provesi, J. G., Dias, C. O., & Amante, E. R. (2011). Changes in carotenoids during processing and storage of pumpkin puree. *Food Chemistry*, 128(1), 195–202.
- Sila, D. N., Van Buggenhout, S., Duvetter, T., Fraeye, I., De Roeck, A., Van Loey, A., & Hendrickx, M. (2009). Pectins in processed fruits and vegetables: Part II—Structure–function relationships. *Comprehensive Reviews in Food Science and Food Safety*, 8(2), 86–104.
- Simal, S., Femenia, A., Garau, M. C., & Rossello, C. (2005). Use of exponential, Page's and diffusional models to simulate the drying kinetics of kiwi fruit. *Journal of Food Engineering*, 66(3), 323–328.
- Sojak, M., & Głowacki, S. (2010). Analysis of giant pumpkin (*Cucurbita maxima*) drying kinetics in various technologies of convective drying. *Journal of Food Engineering*, 99(3), 323–329.
- Song, J., Wang, X., Li, D., Meng, L., & Liu, C. (2017). Degradation of carotenoids in pumpkin (*Cucurbita maxima* L.) slices as influenced by microwave vacuum drying. *International Journal of Food Properties*, 20(7), 1479–1487.
- Tatemoto, Y., Mibu, T., Yokoi, Y., & Hagimoto, A. (2016). Effect of freezing pretreatment on the drying characteristics and volume change of carrots immersed in a fluidized bed of inert particles under reduced pressure. *Journal of Food Engineering*, 173, 150–157.
- Vaccarezza, L. M., Lombardi, J. L., & Chirife, J. (1974). Kinetics of moisture movement during air drying of sugar beet root. *International Journal of Food Science & Technology*, 9(3), 317–327.
- Watanabe, T., Ando, Y., Orikasa, T., Shiina, T., & Kohyama, K. (2017). Effect of short time heating on the mechanical fracture and electrical impedance properties of spinach (*Spinacia oleracea* L.). *Journal of Food Engineering*, 194, 9–14.
- Watanabe, T., Nakamura, N., Ando, Y., Kaneta, T., Kitazawa, H., & Shiina, T. (2018). Application and simplification of cell-based equivalent circuit model analysis of electrical impedance for assessment of drop shock bruising in Japanese pear tissues. *Food and Bioprocess Technology*, 11(11), 2125–2129.
- Wu, L., Ogawa, Y., & Tagawa, A. (2008). Electrical impedance spectroscopy analysis of eggplant pulp and effects of drying and freezing-thawing treatments on its impedance characteristics. *Journal of Food Engineering*, 87(2), 274–280.
- Xiang, Z., Ye, F., Zhou, Y., Wang, L., & Zhao, G. (2018). Performance and mechanism of an innovative humidity-controlled hot-air drying method for concentrated starch gels: A case of sweet potato starch noodles. *Food Chemistry*, 269, 193–201.
- Yang, X., Zhao, Y., & Lv, Y. (2007). Chemical composition and antioxidant activity of an acidic polysaccharide extracted from *Cucurbita moschata* Duchesne ex Poir. *Journal of Agricultural and Food Chemistry*, 55(12), 4684–4690.
- Yang, H., Wu, Q., Ng, L. Y., & Wang, S. (2017). Effects of vacuum impregnation with calcium lactate and pectin methylesterase on quality attributes and chelate-soluble pectin morphology of fresh-cut papayas. *Food and Bioprocess Technology*, 10(5), 901–913.
- Zhang, M. I. N., & Willison, J. H. M. (1992). Electrical impedance analysis in plant tissues: The effect of freeze thaw injury on the electrical properties of potato tuber and carrot root tissues. *Canadian Journal of Plant Science*, 72(2), 545–553.
- Zhang, M. I. N., Willison, J. H. M., Cox, M. A., & Hall, S. A. (1993). Measurement of heat injury in plant tissue by using electrical impedance analysis. *Canadian Journal of Botany*, 71(12), 1605–1611.

**Publisher's Note** Springer Nature remains neutral with regard to jurisdictional claims in published maps and institutional affiliations.